Pergamon

Int. J. Heat Mass Transfer. Vol. 39, No. 3, pp. 527–536, 1996

0017-9310/96 $9.50+0.00

0017-9310(95)00148-4

Studies on molecular diffusion and natural convection in a multicomponent gas system

TETSUAKI TAKEDA and MAKOTO HISHIDA

Nuclear Heat Application System Laboratory, Department of High Temperature Engineering, Japan Atomic Energy Research Institute, Tokai-mura, Ibaraki-ken, 319-11, Japan

(*Received* 16 *December* 1994 *and in final form* 27 *March* 1995)

Abstract—Experimental and numerical studies have been carried out on the combined phenomena of molecular diffusion and natural convection with a graphite oxidation reaction in a multicomponent gas system to investigate the process of air ingress into a reverse U-shaped tube consisting of one side heated and the other side cooled pipes. The range of the Grashof number based on the height of the tube was about $3.7 \times 10^9 < Gr_L < 4.7 \times 10^{11}$. One-dimensional basic equations for continuity, momentum conservation, energy conservation of the gas mixture, and mass conservation of the gas species are numerically solved to obtain concentration changes in the gas species and the onset time of the natural circulation of air. The experimental results showed that air entered the tube due to molecular diffusion and a very weak natural convection of the multicomponent gas mixed prior to the onset of the natural circulation of air. The calculated results are in good agreement with the experimental ones regarding the concentration changes in the gas species and the onset time of the natural circulation of air.

1. INTRODUCTION

A high-temperature engineering test reactor (HTTR) is now in its developmental stage at JAERI [1]. It is a graphite-moderated high-temperature gas-cooled thermal reactor. A schematic drawing of the HTTR and the coolant passages in the reactor are provided in Fig. 1. A hot leg consists of an inner passage of a coaxial duct, a high-temperature outlet duct, a high-temperature plenum and fuel cooling channels. A cold leg consists of an annular passage of the coaxial duct, a bottom cover and an annular passage between the reactor vessel and permanent reflector. As the hot and cold legs are connected at the top cover, they make a kind of reverse U-shaped tube. A primary-pipe rupture accident is one of the most common of accidents related to the basic design of the HTTR. When a primary-pipe rupture accident occurs, the high-pressure helium gas coolant in the reactor is forced out into the reactor container through the breach. Gas pressure should become balanced between the inside and outside of the reactor vessel after a few minutes. During this stage, called the depressurization stage, air is not able to enter the reactor core from the breach. After the depressurization stage, it is supposed that air enters the reactor core from the breach due to molecular diffusion and natural convection of a multicomponent gas mixture induced by the distribution of gas temperature and the resulting concentrations in the reactor. It seems possible that carbon monoxide (CO) and dioxide (CO_2) are produced in the reactor, because the oxygen (O_2) contained in air reacts with the graphite structures. Density of the gas mixture in the reactor gradually increases as air enters by the molecular diffusion and natural convection of the gas mixture in the first stage of the accident. Finally, the second stage of the accident starts after natural circulation of the air occurs suddenly throughout the entire reactor [2].

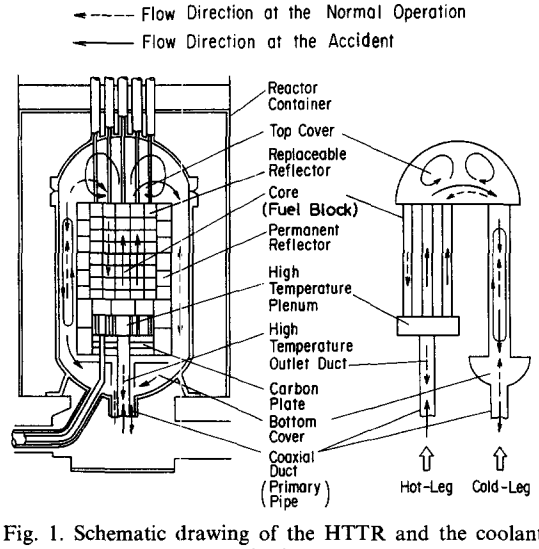

Fig. 1. Schematic drawing of the HTTR and the coolant passages in the reactor.

Previous studies focused mostly on molecular diffusion and natural convection of the two-component gas mixture in a reverse U-shaped tube and in a simple test model of the HTTR [3, 4]. A one-dimensional flow network model was employed to calculate the transport of air into the simple test model simulating the HTTR. The numerical results were in good agreement with the experimental ones regarding

NOMENCLATURE

A production ratio
A_e cross sectional area of tube
C molar density
c_p specific heat capacity at constant pressure
D_{i-j} mutual diffusion coefficient
D_{i-m} effective diffusion coefficient of multicomponent gas mixture system
D_e diameter of tube
E_0, E_1, E_2 activation energy
f friction factor
Gr_L Grashof number based on the height of the tube
g acceleration of gravity
K pressure loss coefficient
K_0, K_1, K_2 reaction constant
L_h length of heated periphery
M molecular weight
N mole number
p fluid static pressure
p_{O_2} partial pressure of oxygen
Q production and dissipation term
R gas constant
Re Reynolds number based on the diameter of tube
T gas temperature
T_w wall temperature
t time
u mass average velocity
X mole fraction of component gas
x co-ordinate or distance from tube inlet.

Greek symbols
α heat transfer coefficient
θ inclination of flow direction
λ thermal conductivity
μ viscosity
ν kinematic viscosity
ρ density
ω mass fraction.

Subscripts
C carbon
CO carbon monoxide
CO_2 carbon dioxide
He helium
i i component gas
m gas mixture
N_2 nitrogen
O_2 oxygen.

the concentration change in the gas species and the onset time of the natural circulation of air. According to the results obtained [4], the density of the gas mixture in the reverse U-shaped tube gradually increases as nitrogen(N_2) enters as a result of molecular diffusion and because of very weak natural convection. The calculated velocity of this very weak natural convection of the gas mixture is about $10^{-6} \sim 10^{-3}$ m s^{-1} ($10^{-4} < Re < 1$). The natural circulation of N_2, which is larger than 0.1 m s^{-1} ($Re > 100$), occurs suddenly throughout the reverse U-shaped tube, because the buoyancy force has risen to such an extent as to bring about natural circulation. However, with these previous test rigs, we were not able to observe the behavior of the multicomponent gas mixture with the graphite oxidation reaction, because the test models were lacking graphite structures.

The objectives of this present study is to investigate the basic features of the flow behavior of the multicomponent gas mixture, consisting of He, N_2, O_2, CO_2, CO, etc. This paper concentrates on experimental and numerical studies regarding the combined phenomena of the molecular diffusion and the natural convection of the multicomponent gas mixture with the graphite oxidation reaction in the reverse U-shaped tube [5]. One-dimensional basic equations for continuity, momentum conservation, energy conservation of the gas mixture, and the mass conservation of gas species are numerically solved to obtain the concentration change in the gas species and the onset time of the natural circulation of air in the reverse U-shaped tube. The numerical results are compared with the experimental ones regarding the density of the gas mixture, the concentration of each gas species produced by the graphite oxidation reaction and the onset time of the natural circulation of air.

2. NUMERICAL ANALYSIS

2.1. *Basic equations*

The analytical model of the reverse U-shaped tube can be seen in Fig. 2. The reverse U-shaped tube is made up of channels where one side is heated and the other cooled. The cross-sectional area of the tube is constant. The numerical analysis is made under the following assumptions:

(1) one-dimensional laminar flow;
(2) a diffusion coefficient of each component gas ($D_{i\text{-}m}$) for the multicomponent gas system is a function of the temperature, pressure and the mole fraction of gas species;
(3) each gas species and the gas mixture follow the equation of state for ideal gas and
(4) a chemical reaction between carbon and oxygen, and a carbon monoxide combustion are taken into consideration.

The basic equations are as follows.

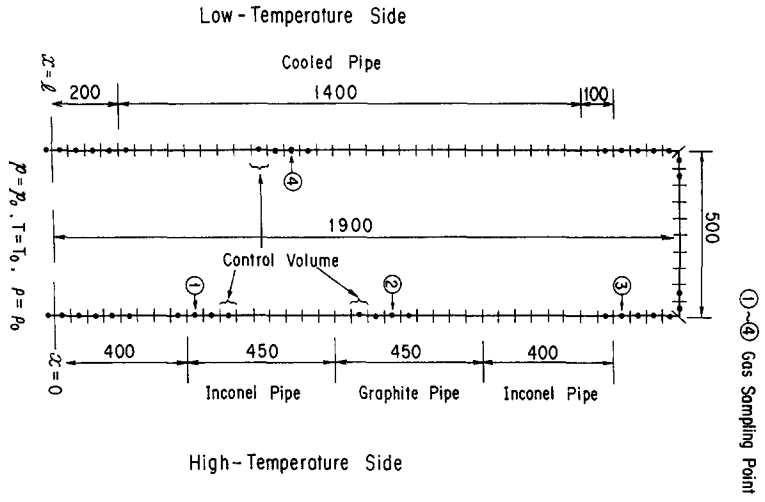

Fig. 2. Analytical model of the reverse U-shaped tube.

The equation of continuity for the gas mixture:

$$\frac{\partial \rho}{\partial t}+\frac{\partial(\rho u)}{\partial x}=\sum Q_i. \tag{1}$$

The equation of continuity for each gas species (species i):

$$\frac{\partial(\rho\omega_i)}{\partial t}+\frac{\partial(\rho\omega_i u)}{\partial x}=\frac{\partial}{\partial x}\left(\rho D_{i\text{-m}}\frac{\partial \omega_i}{\partial x}\right)+Q_i. \tag{2}$$

The equation of momentum conservation:

$$\rho\frac{\partial u}{\partial t}+\rho u\frac{\partial u}{\partial x}=-\frac{\partial p}{\partial x}-\rho g\cos\theta-\tfrac{1}{2}\rho u|u|\left(\frac{f}{D_e}+K\right). \tag{3}$$

The equation of energy conservation:

$$\frac{\partial(\rho c_p T)}{\partial t}+\frac{\partial(\rho u c_p T)}{\partial x}=\frac{\partial}{\partial x}\left(\lambda\frac{\partial T}{\partial x}\right)+\alpha\frac{L_h}{A_e}(T_w-T). \tag{4}$$

The equation of state for the gas:

$$p=\frac{\rho}{M}RT. \tag{5}$$

Here, the diffusion coefficients for the multicomponent gas system are obtained from the diffusion coefficients for the binary gas system and the mole fractions of each gas species.

$$D_{i-\text{m}}=\frac{1-X_i}{\sum_{j=1}^{n}\frac{X_j}{D_{i-j}}}. \tag{6}$$

This coefficient is called the effective diffusion coefficient in the multicomponent gas mixture, which is provided by Wilke [6]. Fairbanks and Wilke [7], and Walker *et al.* [8] reported that the effective diffusion coefficient given by equation (6) agreed well with the experimental data for the three-component gas mixture.

Angle θ is an inclination of the flow direction, and θ is zero when the flow is vertically upwards. x is an axial distance in the tube and the positive direction of x is equal to the positive direction of u. Friction factor (f) and heat transfer coefficient (α) corresponding to the fully developed laminar flow are used [9] and pressure loss coefficient (K) is assumed to be 1.0 at the inlet and outlet of the reverse U-shaped tube. Viscosity (μ) and thermal conductivity (λ) of each gas species and gas mixture is obtained using the Wilke method [10] and by the Eucken correlation [11], respectively. Density (ρ) of each gas species and the gas mixture is calculated from Ref. [11].

2.2. *Graphite oxidation reaction*

In the present analysis, the graphite oxidation reaction (C–O_2 reaction) and the carbon monoxide combustion (CO–O_2 reaction) are taken into account. The chemical equation of the graphite oxidation reaction is expressed as

$$C+zO_2\rightarrow xCO+yCO_2. \tag{7}$$

A reaction rate is described as

$$r_{C\text{-}O}=K_0\exp\left(-\frac{E_0}{RT}\right)p_{O_2}^n. \tag{8}$$

Though a large number of an activation energy and a reaction constant are reported [12], we have used the following values that interporate the experimental data for IG-110 in Ref. [13].

$$K_0=3.60\times10^2$$

$$E_0=2.09\times10^2\quad[\text{kJ mol}^{-1}].$$

Here, K_0 is the reaction constant, E_0 the activation energy and p_{O_2} the oxygen partial pressure. The unit of R, T, $r_{C\text{-}O}$ and p_{O_2} are [J mol^{-1} K^{-1}], [K], [kg kg^{-1} s^{-1}]

and [Pa], respectively. The value of the exponential index, n, in terms of the oxygen partial pressure ranges from 0.75 to 1 for PGX in Ref. [13]. We have adopted 1.0 for the value of the exponential index in this analysis, because we have no data for IG-110.

A production ratio of CO to CO_2 ($x/y = A$) is correlated as follows:

$$A = K_1 \exp\left(-\frac{E_1}{RT}\right) \tag{9}$$

where K_1 is the constant and E_1 the activation energy. There are many previous reports [14–16] regarding the production ratio. However, the reported ratios differ over a wide range because the production ratio depends on experimental conditions, for example, the catalytic effect of the impurities contained in the graphite and the grade of graphite. In the preliminary calculation, the following three sets of the reported values for K_1 and E_1 have been tested to find the optimum one.

$K_1 = 2.512 \times 10^3$, $E_1 = 5.191 \times 10^1$ [kJ mol^{-1}] from Ref. [14]

$K_1 = 7.943 \times 10^3$, $E_1 = 7.83 \times 10^1$ [kJ mol^{-1}] from Ref. [15]

$K_1 = 1.995 \times 10^3$, $E_1 = 5.986 \times 10^1$ [kJ mol^{-1}] from Ref. [15].

It was revealed that the calculated results using the second set of K_1 and E_1 agreed well with the experimental results much better than those using the first and third sets of K_1 and E_1. The calculated results using the first and third sets of K_1 and E_1 gave a higher CO concentration and lower CO_2 concentration than the measured concentrations. In the present calculation, the second set of K_1 and E_1 was used. Consequently, the mole number for the dissipation term of O_2 and for the generation terms of CO and CO_2 can be obtained from the following relation, respectively.

$$z = N_{O_2} = \frac{A+2}{2(A+1)} \tag{10}$$

$$x = N_{CO} = \frac{A}{A+1} \tag{11}$$

$$y = N_{CO_2} = \frac{1}{A+1}. \tag{12}$$

Therefore, the dissipation and generation terms in the equations of the mass conservation for each component gas species can be rewritten as follows:

O_2 dissipation term

$$Q'_{O_2} = -N_{O_2} r_{C\text{-}O} \frac{\rho_C}{M_C} M_{O_2} \text{ [kg m}^{-3}\text{ s}^{-1}\text{]} \tag{13}$$

CO generation term

$$Q'_{CO} = N_{CO} r_{C\text{-}O} \frac{\rho_C}{M_C} M_{CO} \text{ [kg m}^{-3}\text{ s}^{-1}\text{]} \tag{14}$$

CO_2 generation term

$$Q'_{CO_2} = N_{CO_2} r_{C\text{-}O} \frac{\rho_C}{M_C} M_{CO_2} \text{ [kg m}^{-3}\text{ s}^{-1}\text{]} \tag{15}$$

where ρ_C is the density of the graphite material and M_C is the mole weight of carbon.

The chemical equation of the CO combustion is expressed as

$$CO + \tfrac{1}{2}O_2 \rightarrow CO_2. \tag{16}$$

The reaction rate was taken from Ref. [17]

$$\frac{dC_{CO}}{dt} = -r_{CO\text{-}O_2} \cdot C_{CO} \cdot C_{O_2}^{0.5} \cdot C_{H_2O}^{0.5} \text{ [mol m}^{-3}\text{ s}^{-1}\text{]} \tag{17}$$

where

$$r_{CO\text{-}O_2} = K_2 \exp\left(-\frac{E_2}{RT}\right). \tag{18}$$

$$C_{CO} = \frac{\rho_{CO}}{M_{CO}} = \frac{\rho \cdot \omega_{CO}}{M_{CO}} \tag{19}$$

$$C_{O_2} = \frac{\rho_{O_2}}{M_{O_2}} = \frac{\rho \cdot \omega_{O_2}}{M_{O_2}} \tag{20}$$

$$C_{H_2O} = C \cdot X_{H_2O} = \frac{\rho}{M} \cdot X_{H_2O}. \tag{21}$$

Here, $K_2 = 1.3 \times 10^8$ [m^3 mol^{-1} s^{-1}], $E_2 = 126$ [kJ mol^{-1}] and $X_{H_2O} = 0.0054 \pm 0.0007$ [18]. Therefore, the dissipation or generation terms of CO, CO_2 and O_2 are

$$Q''_{CO} = \frac{dC_{CO}}{dt} M_{CO} = -r_{CO\text{-}O_2} \cdot X_{H_2O}^{0.5} \cdot \rho \left(\frac{\rho^2}{M \cdot M_{O_2}}\right)^{0.5} \omega_{CO} \omega_{O_2}^{0.5} \text{ [kg m}^{-3}\text{ s}^{-1}\text{]} \tag{22}$$

$$Q''_{O_2} = -0.5 \frac{dC_{CO}}{dt} M_{O_2} = -0.5 r_{CO\text{-}O_2} \cdot X_{H_2O}^{0.5} \cdot \rho \left(\frac{\rho^2}{M \cdot M_{O_2}}\right)^{0.5} \omega_{CO} \omega_{O_2}^{0.5} \frac{M_{O_2}}{M_{CO}} \text{ [kg m}^{-3}\text{ s}^{-1}\text{]} \tag{23}$$

$$Q''_{CO_2} = \frac{dC_{CO}}{dt} M_{CO_2} = r_{CO\text{-}O_2} \cdot X_{H_2O}^{0.5} \cdot \rho \left(\frac{\rho^2}{M \cdot M_{O_2}}\right)^{0.5} \omega_{CO} \omega_{O_2}^{0.5} \frac{M_{CO_2}}{M_{CO}} \text{ [kg m}^{-3}\text{ s}^{-1}\text{]}. \tag{24}$$

Finally, the dissipation or generation terms of the mass conservation equations for O_2, CO and CO_2 are written as

$$Q_{O_2} = Q'_{O_2} + Q''_{O_2} \tag{25}$$

$$Q_{CO} = Q'_{CO} + Q''_{CO} \tag{26}$$

$$Q_{CO_2} = Q'_{CO_2} + Q''_{CO_2}. \quad (27)$$

2.3. *Discretization of the basic equations*

As shown in Fig. 2, the analytical region is divided into 88 control volumes using a staggered grid. Thus, the velocity is calculated for the points that lie on the control-volume faces and the density, temperature, mole fraction and pressure are defined at the center in the control volume. We also have adopted a donor-cell method for discretization of the basic equations. The equations of continuity for the gas mixture, momentum and energy conservation for the gas mixture, and mass conservation for each component gas are solved using a fully implicit scheme.

The initial conditions for the multicomponent gas system are as follows. He is initially put in the reverse U-shaped tube with the outside being air. Air is assumed to be a binary gas mixture of N_2 and O_2. That is,

mole fraction X at $t = 0$;

$0 < x < 1$ (in the reverse U-shaped tube),

$$X_{N_2}, X_{O_2}, X_{CO}, X_{CO_2} = 0, X_{He} = 1. \quad (28)$$

$x = 0, 1$ (at the both ends of the tube),

$$X_{N_2} = 0.791, X_{O_2} = 0.209, X_{CO}, X_{CO_2}, X_{He} = 0. \quad (29)$$

The initial velocity is zero for all the control-volume faces. Gas pressure is assumed to be constant at atmospheric pressure. Wall temperature in the reverse U-shaped tube is set to equal for the measured wall temperature. Figure 3 shows a typical example of the measured wall temperature distribution regarding the whole tube. To simulate the fundamental features of the temperature distribution in the reactor, it is desirable that the temperature distribution of the high-temperature side pipe be set to a flat temperature. Although the flat temperature distribution could not be achieved because the connecting parts between the vertical and horizontal pipes were not heated, the present temperature distribution shown in Fig. 3 was sufficient to investigate the basic features of the flow

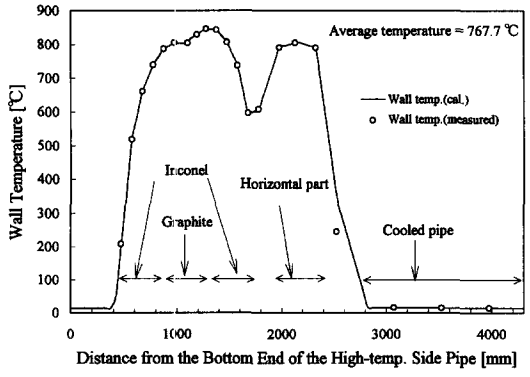

Fig. 3. Distribution of the measured wall temperature in the whole tube.

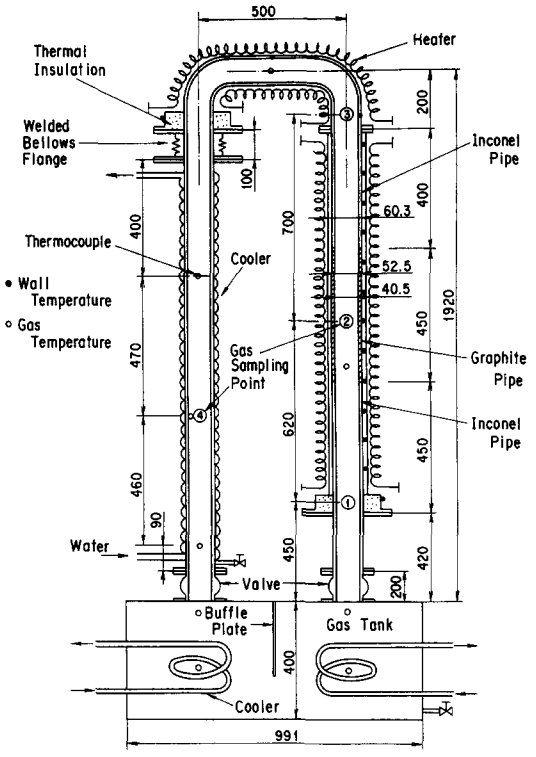

Fig. 4. Experimental apparatus.

behavior of the multicomponent gas mixture with the graphite oxidation reaction.

The boundary conditions are:

$$\text{at } x = 0 \text{ and } x = 1, \quad X_{N_2} = 0.791, \quad X_{O_2} = 0.209,$$

$$X_{CO}, \quad X_{CO_2}, \quad X_{He} = 0, \quad p = p_0, \quad T = T_0, \quad \rho = \rho_0. \quad (30)$$

3. EXPERIMENTAL APPARATUS AND PROCEDURES

A rough sketch of the experimental apparatus can be seen in Fig. 4. The apparatus consists of a reverse U-shaped tube and a gas tank. One vertical pipe is heated using electrical power and the other vertical one is cooled by water. A horizontal and two bent pipes, connecting these two vertical pipes, are also heated. The vertical heated pipe, made of inconel, has an inner diameter of 52.5 mm, an outer diameter of 60.3 mm and a length of 1300 mm. A graphite pipe is inserted into the inconel heated pipe and it measures 40.5 mm i.d., 52.5 mm o.d. and 450 mm in length. The graphite, IG-110, is from Toyo Tanso Co. The upper and lower inner pipes, which are also inserted in the heated pipe, are made of inconel and have the same diameter as the graphite pipe. The horizontal and bent pipes have an inner diameter of 40.5 mm. The vertical cooled pipe measures 41.2 mm i.d. and 1420 mm in length. A gas tank, cylindrical in shape, has an i.d. of 991 mm and a height of 400 mm.

The mole fraction of each gas species and the density of the gas mixture were measured at four sampling points shown in Fig. 4. The density of the gas mixture, the mole fraction of O_2, CO and CO_2 were measured using a gas analyzer (Yokogawa: density-Vibro gas analyzer DG8, O_2-Electrochemical analyzer 6234, CO and CO_2-Infrared rays analyzer IR21). The output signals of the mole fraction of CO and CO_2 for N_2 based gas were higher than those for He based gas in the infrared rays analyzer. Therefore, the results of the mole fraction of CO and CO_2 were corrected using the following method.

The gas mixture in the apparatus was assumed to be a helium–air binary gas mixture. Then, the mole fraction of air was obtained from the following equation:

$$X_{\text{air}} = \frac{\rho - \rho_{\text{He}}}{\rho_{\text{air}} - \rho_{\text{He}}} \tag{31}$$

where X_{air} is mole fraction of air based on helium–air binary gas mixture; ρ, density of gas mixture obtained from the analyzer; ρ_{He}, density of helium at 1 atm, 20°C; ρ_{air}, density of air at 1 atm, 20°C.

The corrected mole fractions of CO_2 ($X_{\text{CO}_2/\text{real}}$) and CO ($X_{\text{CO/real}}$) were obtained as

$$X_{\text{CO}_2/\text{real}} = (1 - X_{\text{air}})X_{\text{CO}_2/\text{He}} + X_{\text{air}} \cdot X_{\text{CO}_2/\text{N}_2} \tag{32}$$

$$X_{\text{CO/real}} = (1 - X_{\text{air}})X_{\text{CO/He}} + X_{\text{air}} \cdot X_{\text{CO/N}_2} \tag{33}$$

where $X_{\text{CO}_2/\text{He}}$ and $X_{\text{CO}_2/\text{N}_2}$ are the mole fraction of CO_2 obtained from the calibration results for He and N_2 based gas, and $X_{\text{CO/He}}$ and $X_{\text{CO/N}_2}$ are the mole fraction of CO obtained from the calibration results for He and N_2 based gas, respectively.

The temperature distribution of the pipe wall was measured by 18 K-type thermocouples and the temperatures of the gas mixture were also measured at nine points using K-type thermocouples at the positions indicated in Fig. 4 using black circles and white circles, respectively. The signals of the voltage from the thermocouples and the gas analyzer were digitally sampled and read using a data acquisition control unit (Scanner and DVM: Advantest TR2730 & TR2731). These units were controlled by a Hewlett-Packard Series 9000 Model 216 computer. We assumed that the onset time of the natural circulation of air is the time when the gas temperature at the cooled pipe exceeds 100°C. As the natural circulation of N_2 occurs, the gas temperature at the upper part of the cooled pipe increases rapidly. The time required for the gas temperature to be increased from 20 to 100°C is about 10 s.

In consideration of the errors induced by the thermocouples, scanner junction and DVM accuracy, the entire accuracy of the temperature measurement was within ±0.3°C. The measurements accuracy of the density analyzer and the concentration analyzer (O_2, CO, CO_2) were ±1% F.S. and ±1.7% F.S., respectively. The relative uncertainty in the density of the gas mixture was found to be ±4%. The uncertainties in the mole fraction of O_2, CO and CO_2 were found to be ±2.3%, ±4.4% and ±4.4%, respectively. The uncertainty in the onset time of the natural circulation of air was estimated to be 12%.

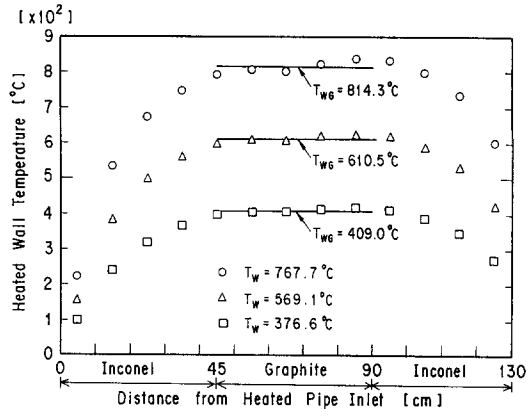

Fig. 5. Distribution of the measured wall temperature in the heated pipe.

Experimental procedures are as follows. The ball valves between the reverse U-shaped tube and the gas tank were closed and the tube was evacuated using a vacuum pump. Helium and air was injected into the tube and the gas tank, respectively. Then, the high-temperature side pipe and the connecting pipe were heated from about 400 to 800°C (the longitudinal average temperature of the high-temperature side pipe). When the temperature of the gas and the pipe wall reached a steady-state condition, the gas pressure in the reverse U-shaped tube was equalized to the atmospheric pressure by the opening a small release valve. Then, the two ball valves were open at the same time to simulate a pipe rupture accident. During the experiment, the temperature change of the pipe wall was held within ±2°C.

4. EXPERIMENTAL AND NUMERICAL RESULTS

Figure 5 provides examples of the wall temperature distribution of the heated pipe for the various average temperatures. The temperature of the graphite part has a flat temperature distribution, because the graphite pipe is inserted in the center position of the heated pipe. The solid lines show the average temperatures of the graphite pipe. The longitudinal average temperatures of the whole heated pipe are about 40° lower than those of the graphite pipe. The longitudinal average temperatures of the whole heated pipe and the graphite pipe are shown in Table 1. The range of the Grashof number based on the height of the reverse U-shaped tube was about $3.7 \times 10^9 < Gr_L < 4.7 \times 10^{11}$ in the present experiment.

Figure 6 shows the relationship between the onset time of the natural circulation of air and the average temperature of the heated pipe. When the average temperature of the heated pipe ranges from 450 to 650°C, the onset time of the natural circulation in the

Table 1. Longitudinal average temperatures of the whole heated pipe and graphite pipe

Whole heated pipe [°C]	811	767.7	715.4	661.8	618.1	569.1	523.5	466.2	423.8	376.6
Graphite pipe [°C]	859.1	814.3	760	708.2	660.8	610.5	562.9	508	460.3	409

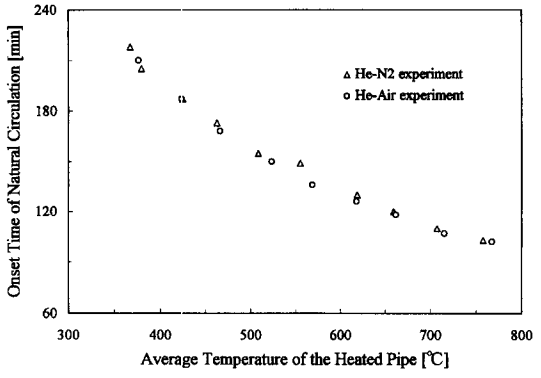

Fig. 6. Relationship between the onset time of natural circulation and the average temperature of the heated pipe.

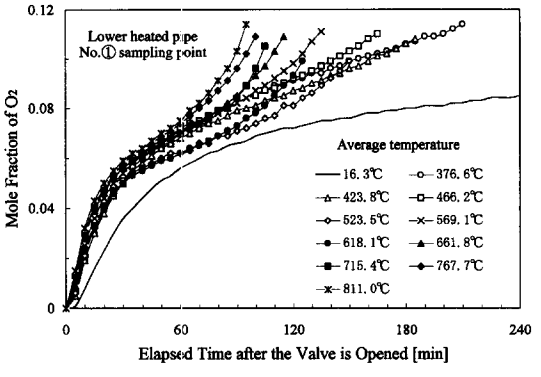

Fig. 7. Measured mole fraction change of O_2 in the lower part of the heated pipe.

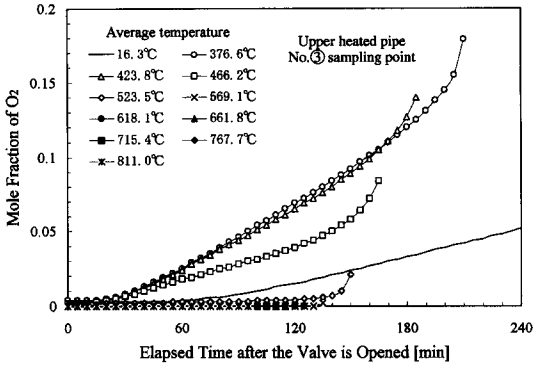

Fig. 8. Measured mole fraction change of O_2 in the upper part of the heated pipe.

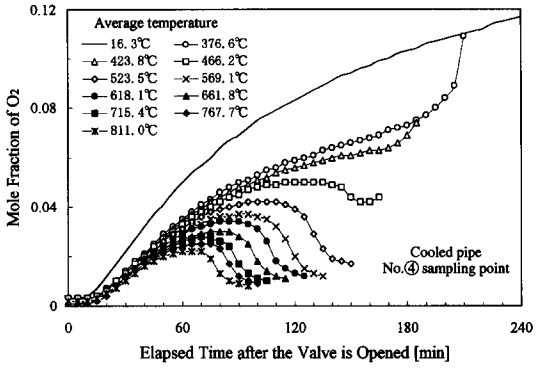

Fig. 9. Measured mole fraction change of O_2 in the cooled pipe.

He–air cases is slightly earlier than that in the He–N_2 cases. This is due to the fact that the density of the gas mixture throughout the whole apparatus becomes larger as a result of the production of CO_2 [19].

Figures 7–9 show the measured mole fraction changes of O_2 in the lower part of the heated pipe (sampling point ①), the upper part of the heated pipe (sampling point ③) and the cooled pipe (sampling point ④), respectively, for various longitudinal average temperatures of the heated pipe. The solid lines in the figures are the experimental results when the reverse U-shaped tube was kept at the room temperature (isothermal experiment, 16.3°C). The measured mole fraction of O_2 at sampling point ① in the case of the non-isothermal experiments increased faster than that in the case of the isothermal one. This is because O_2 is transported by a very weak natural convection of the gas mixture in addition to by the molecular diffusion. On the other hand, the measured mole fraction of O_2 at sampling point ④ of the cooled pipe in the non-isothermal cases is lower than that in the isothermal one, because the amount of O_2 transported downward by the very weak natural convection is larger than that transported upward by the molecular diffusion. As the reaction rate of the graphite oxidation reaction increases as the temperature increases, the measured mole fractions of O_2 at sampling points ③ and ④ decrease with an increase in the temperature of the graphite pipe. When the average temperature of the heated pipe is higher than 523.5°C (graphite temperature = 562.9°C), O_2 almost dissipates as a result of the graphite oxidation reaction at the graphite part. Therefore, the mole fraction of O_2 is almost zero in the upper part of the heated pipe. The measured mole fraction of O_2 at the cooled pipe first increases with time, because the amount of O_2 transported upward by the molecular diffusion is larger than that transported downward by the very weak natural convection of the gas mixture. However, because O_2 is dissipated in the graphite part and is not contained in the natural convection of the gas mixture when the

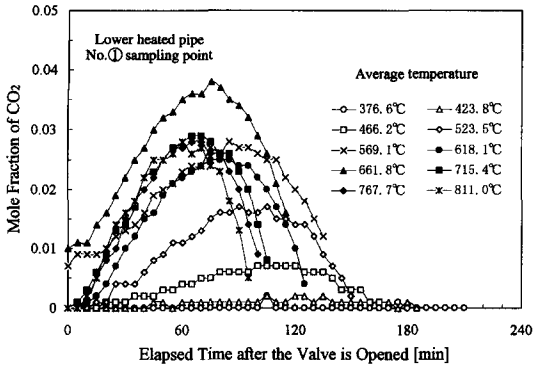

Fig. 10. Measured mole fraction change of CO_2 in the lower part of the heated pipe.

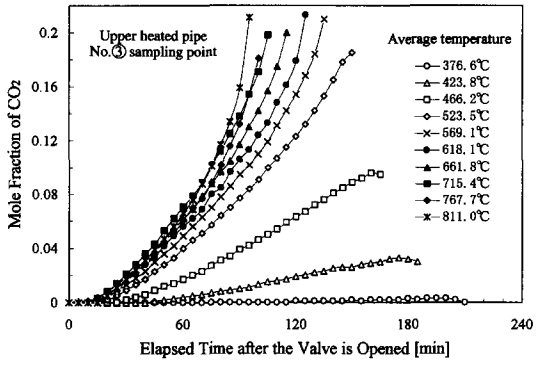

Fig. 11. Measured mole fraction change of CO_2 in the upper part of the heated pipe.

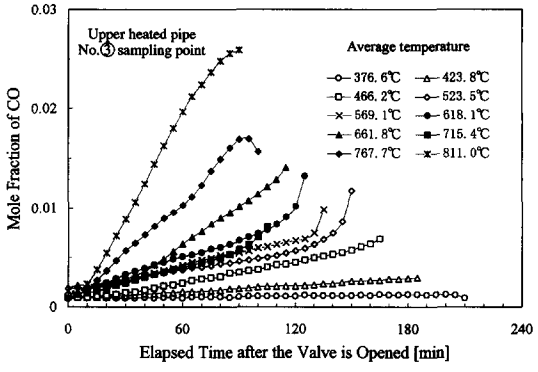

Fig. 12. Measured mole fraction change of CO in the upper part of the heated pipe.

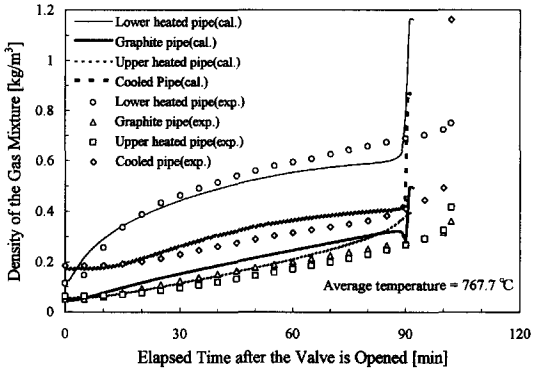

Fig. 13. Density change of the gas mixture (average temperature = 767.7°C).

average temperature of the heated pipe is higher than 523.5°C, the mole fraction of O_2 in the cooled pipe decreases with time and approaches zero just before the natural circulation of air begins.

Figures 10 and 11 show the measured mole fraction change of CO_2 in the lower part of the heated pipe (sampling point ①) and the upper part of the heated pipe (sampling point ③), respectively. The measured mole fraction change of CO_2 in sampling point ① first increases gradually with time, because the CO_2 generating in the graphite part is transported downward due to the molecular diffusion. As the upward velocity of the natural convection of the gas mixture becomes larger, however, the mole fraction of CO_2 decreases with time. On the other hand, the measured mole fraction change of CO_2 in sampling point ③ increases with time until the natural circulation of air begins. When the average temperature of the heated pipe is lower than 376.6°C (graphite temperature = 409°C), CO_2 is not detected because of the very small reaction rate of the graphite oxidation reaction. Figure 12 shows the measured mole fraction change of CO in the upper part of the heated pipe (sampling point ③). The mole fraction of CO was very small (lower than 0.03) for all of the experiments, because the production ratio of CO to CO_2 was small. According to equation (9), production ratio (A) was greater than 1 when the temperature exceeded 780°C.

Figure 13 shows the typical density changes of the gas mixture at the various gas sampling points when the average temperature of the graphite pipe is 767.7°C (graphite temperature = 814.3°C). Symbols (○, △, □ and ◇, respectively) represent the measured density changes at the gas sampling positions (①–④). The solid and dotted lines in the figure are the results obtained from the present calculation. As the density of the gas mixture in the tube gradually increases, the buoyancy force also increases. When the average temperature is 767.7°C, the buoyancy force becomes large enough to initiate the natural circulation of air throughout the reverse U-shaped tube at around 105 min after the valve is opened. The onset time of the natural circulation of air in this analysis is about 90 min after the valve is opened. Before the onset of the natural circulation of air, the calculated velocity of the very weak natural convection of the gas mixture was about $1 \times 10^{-6} < u < 1 \times 10^{-3}$ m s^{-1} ($1 \times 10^{-4} < Re < 1$) at the inlet of the reverse U-shaped tube. The calculated velocity of this natural convection was very slow in comparison with that of the natural circulation of air, which was around 1.4×10^{-1} m s^{-1} ($Re = 450$). The calculated results of the density change and the onset time of the natural circulation of air were in good agreement with the experimental ones. The difference in the onset time of

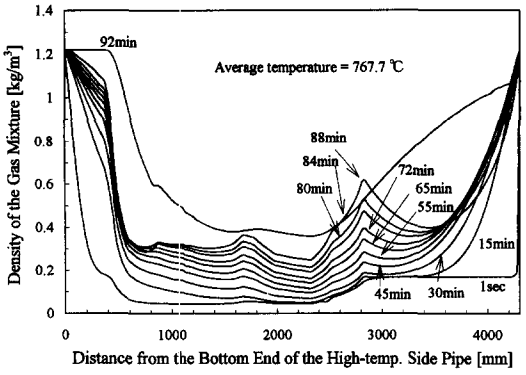

Fig. 14. Distribution of the density change of the gas mixture along the x-axis direction (average temperature = 767.7°C).

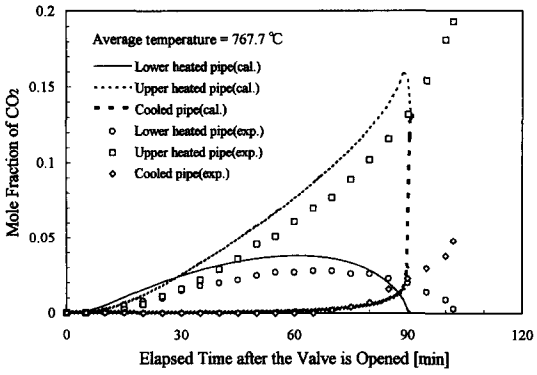

Fig. 16. Mole fraction change of CO_2 (average temperature = 767.7°C).

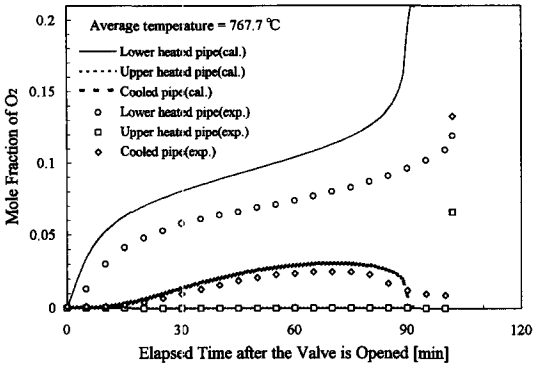

Fig. 15. Mole fraction change of O_2 (average temperature = 767.7°C).

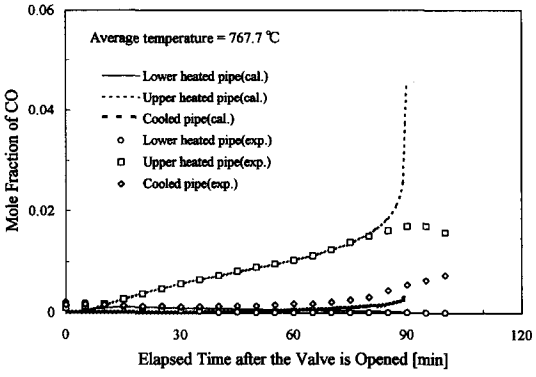

Fig. 17. Mole fraction change of CO (average temperature = 767.7°C).

the natural circulation of air was within 15% between the calculation and the experiment. Figure 14 shows the distribution of the calculated density of the gas mixture along the x-axis direction, when the average temperature of the graphite pipe was 767.7°C. As shown in the figure, the density of the gas mixture in the low-temperature-side pipe is larger than that in the high-temperature-side pipe. The density distribution in the whole tube is complicated because the density of the gas mixture is affected not only by the temperature but also by the concentration of each of the gas species.

Figure 15 shows the measured and calculated mole fraction changes of O_2 at the various gas sampling points. The calculated mole fraction changes of O_2 are in good agreement with the experimental ones. The calculated mole fraction of O_2 was higher than the experimental one in the lower part of heated pipe (Ⓘ). The difference in the mole fraction of O_2 between the measured and the calculated results was within 10%. Figures 16 and 17 show the measured and calculated mole fraction changes of CO_2 and CO when the average temperature of the heated pipe was 767.7°C. The calculated mole fraction of CO_2 was slightly higher than the experimental one in the lower part of heated pipe (Ⓘ). The calculated mole fractions of CO were in good agreement with the experimental ones. Figures 18 and 19 show the distribution of the calculated mole fraction of CO_2 and CO along the x-axis direction. As shown in Figs. 18 and 19, the mole fraction of CO_2 and CO had its maximum value at the inlet of the graphite pipe. CO_2 is transported downward by the molecular diffusion against the very weak natural convection of the gas mixture. CO is also transported downward, but the mole fraction of CO in the lower part of the heated pipe is nearly zero due to the CO combustion reaction.

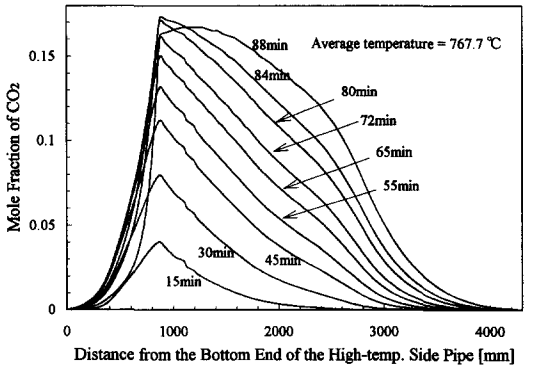

Fig. 18. Distribution of the mole fraction change of CO_2 along the x-axis direction (average temperature = 767.7°C).

To get an even better agreement regarding the

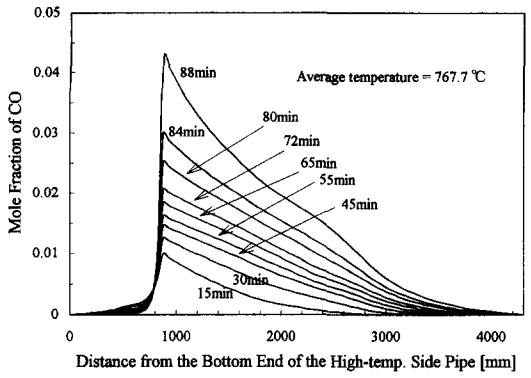

Fig. 19. Distribution of the mole fraction change of CO along the x-axis direction (average temperature = 767.7°C).

amount of the produced gases by the graphite oxidation reaction between the experimental and numerical results, it is necessary to use more appropriate values regarding the reaction constant and the activation energy for graphite oxidation reaction and for the production ratio of CO to CO_2. In the HTTR, local natural convection takes place in local spaces like the top space of the pressure vessel and the annular passage between the permanent reflector and pressure vessel. Therefore, to analyze the transport process of each type of gas species in the HTTR using this numerical analysis, it is necessary to modify the one-dimensional model. Two- or three-dimensional analysis is still open for future study.

5. CONCLUSIONS

Experimental and numerical studies were performed on the combined phenomena of molecular diffusion and natural convection in a multicomponent gas system with chemical reactions in a reverse U-shaped tube. The following conclusions were obtained.

(1) Before the onset of the natural circulation of air, air enters the reverse U-shaped tube by the molecular diffusion and the natural convection of the multicomponent gas mixture, which is induced by the buoyancy force caused by the density distributions of the gas mixture in the tube.

(2) The density of the gas mixture in the reverse U-shaped tube gradually increases as time elapses after the valve is opened. The natural circulation of air takes place suddenly throughout the reverse U-shaped tube when the buoyancy force becomes large enough for the natural circulation of air to begin.

(3) In the present experiment, when the average temperature of the graphite part is higher than about 560°C, oxygen almost dissipates due to the graphite oxidation reaction. When the average temperature of the graphite pipe exceeds 800°C, the amount of the CO produced increases and the CO produced reacts with O_2.

(4) The calculated results of the density change of the gas mixture, the mole fraction changes of each type of gas species and the onset time of the natural circulation of air agree well with the experimental results. It was found that this numerical analysis code can predict the behavior of each type of gas species and the amount of the gases produced by the graphite oxidation reaction.

Acknowledgements—The authors would like to express their gratitude to Dr M. Ogawa of Japan Atomic Energy Research Institute (JAERI) for his many valuable suggestions concerning graphite oxidation reactions.

REFERENCES

1. S. Saito *et al.*, The second JAERI symposium on HTGR technologies, JAERI-M 92-090, Japan Atomic Energy Research Institute (1992).
2. M. Hishida, M. Fumizawa, T. Takeda, M. Ogawa and S. Takenaka, Researches on air ingress accidents of the HTGR, *Nucl. Engng Des.* **144,** 317–325 (1993).
3. M. Hishida and T. Takeda, Study on air ingress during an early stage of a primary-pipe rupture accident of a high-temperature gas-cooled reactor, *Nucl. Engng Des.* **126,** 175–187 (1991).
4. T. Takeda and M. Hishida, Studies on diffusion and natural convection of two-component gases, *Nucl. Engng Des.* **135,** 341–354 (1992).
5. T. Takeda and M. Hishida, Studies on molecular diffusion and natural convection of multicomponent gases, *Proceedings of Sixth International Topical Meeting on Nuclear Reactor Thermal Hydraulics*, Vol. II, pp. 1489–1497, Grenoble, France, 5–8 October (1993).
6. C. R. Wilke, Diffusional properties of multicomponent gases, *Chem. Engng Prog.* **46,** 95–104 (1950).
7. D. F. Fairbanks and C. R. Wilke, Diffusion coefficients in multicomonent gas mixture, *Ind. Engng Chem.* **42,** 471–475 (1950).
8. R. E. Walker, N. de Haas and A. A. Westenberg, Measurements of multicomponent diffusion coefficients for the CO_2–He–N_2 system using the point source technique, *J. Chem. Phys.* **32,** 1314–1316 (1960).
9. R. K. Shah and A. L. London, *Advances in Heat Transfer: Laminar Flow Forced Convection in Ducts*, p. 78. Academic Press, New York (1978).
10. C. R. Wilke, *J. Chem. Phys.* **18,** 517 (1950).
11. R. C. Reid, J. M. Prausnitz and T. K. Sherwood, *The Properties of Gases and Liquids* (3rd Edn), pp. 37–40, 226, 410–414, 470–474, 548–565. McGraw-Hill, New York (1977).
12. D. E. Baker, Graphite as a neutron moderator and reflector material, *Nucl. Engng Des.* **14,** 413–444 (1970).
13. H. Kawakami, Air oxidation behavior of carbon and graphite materials for HTGR, *TANSO* **124,** 26–33 (1986).
14. J. Arthur, *Trans. Faraday Soc.* **47,** 164 (1956).
15. M. Rossberg, *Z. Elektrochem.* **60,** 952 (1956).
16. R. Phillips, F. J. Vastola and P. L. Walker, Jr, Factors affecting the product ratio of the carbon–oxygen reaction—II. Reaction temperature *Carbon* **8,** 205–210 (1970).
17. J. B. Howard, G. C. Williams and D. H. Fine, Kinetics of carbon monoxide oxidation in postflame gases, *Proceedings of the 14th International Symposium on Combustion*, pp. 975–986. The Combustion Institute, Pittsburgh (1973).
18. C. Bruno, P. M. Walsh, D. Santavicca and F. V. Bracco, High temperature catalytic combustion of CO–O_2–N_2, Ar, He, CO_2–H_2O mixtures of platinum, *Int. J. Heat Mass Transfer* **26,** 1109–1120 (1982).
19. T. Takeda, M. Hishida and S. Baba, JAERI-M 91–179, Japan Atomic Energy Research Institute (1991) (in Japanese).